

# Pressure Induced Thermodynamically Stable and Mechanically Robust Li-rich Unknown Li-Sn Compounds: A Step Towards Improvement of Li-Sn Batteries

Raja Sen and Priya Johari\*

*Department of Physics, School of Natural Sciences, Shiv Nadar University,  
Greater Noida, Gautam Budhha Nagar, UP 201 314, India.*

Volume expansion and elastic softening of Sn anode on lithiation result in mechanical degradation and pulverization of Sn, affecting the overall performance of Li-Sn batteries. It can however be overcome by using exotic high pressure quenched phase as prelithiated reagent. Moreover, it is known that under pressure many unusual stoichiometric which are basically impossible at ambient pressure, can be synthesized, that may even survive the decompression from high to ambient pressure. We therefore have performed a comprehensive study using evolutionary algorithm and density functional theory based simulations to understand the lithiation of Sn anode at pressure ranging from 1 atm to 20 GPa. The ground state structures of all stable and metastable Li-Sn compounds have been identified at ambient and moderate pressures and their properties have been studied to understand the role of pressure in re-defining the reaction mechanism during charging-discharging process in Li-ion batteries. Besides the well-known existing Li-Sn compounds, our studies reveal the existence of five unreported stoichiometries ( $\text{Li}_8\text{Sn}_3$ ,  $\text{Li}_3\text{Sn}_1$ ,  $\text{Li}_4\text{Sn}_1$ ,  $\text{Li}_5\text{Sn}_1$ , and  $\text{Li}_7\text{Sn}_1$ ) and their associated crystal structures at ambient and high pressure. While  $\text{Li}_8\text{Sn}_3$  has been identified as one of the most stable Li-Sn compound in the entire pressure range (1 atm–20 GPa), the pressure induced Li-rich compounds like  $\text{Li}_5\text{Sn}_1$  and  $\text{Li}_7\text{Sn}_1$  have been classified as providing higher theoretical gravimetric capacity of 1129 and 1580 mA h  $\text{g}^{-1}$ , respectively, than the capacity of the known most lithiated phase, i.e.,  $\text{Li}_{17}\text{Sn}_4$  (960 mA h  $\text{g}^{-1}$ ). Most importantly, our calculations show reduction in volume expansion by  $\sim 50\%$  at 20 GPa, and reveal that the application of pressure can reduce the chance of Li plating and improve the mechanical properties, which are desired to make the battery safer and its life longer.

---

\* priya.johari@snu.edu.in, psony11@gmail.com

## I. INTRODUCTION

In recent years, rechargeable lithium-ion batteries (LIBs) have become a robust candidate by playing crucial role in the field of energy conversion and storage systems. The superior properties of LIBs such as high energy density, longer lifespan, lower toxicity, better safety, and design flexibility, have helped them to distinguish from their competitors such as nickel-cadmium and lead acid batteries, and establish them as the prominent choice for the portable electronics devices.[1–3] However, to expand the horizon of their use in green transportations (*e.g.*; electric vehicles, hybrid electric vehicles, and plug-in hybrid vehicles) and smart grid applications, a further optimization of the energy and power density, with an improved cycle life is demanded. This has initiated the search for the next generation electrode materials that can enhance the efficiency as well as durability of the LIBs.[3–5] As per current scenario, the majority of commercial LIBs employ graphitic anode for their outstanding cyclic performance, relative low expenditure, and stable electrochemical properties.[1, 2] But, low specific capacity of graphite ( $372 \text{ mA h g}^{-1}$ ) greatly restricts the potential of LIBs in the applications seeking high capacity and power. The low capacity of graphite anode is primarily due to the geometric restriction of graphite's structure in which six carbon can accommodate only one Li-ion to form the intercalated compound,  $\text{LiC}_6$ . [1, 2, 6] To improve the capacity, metals and semi-metals that can electrochemically form alloys with lithium have therefore been extensively investigated in the recent years, to move from the era of intercalation to integration chemistry, where compounds are built by formation/cleavage of covalent bonds during charge-discharge process.[7–12]

In search of new anode materials, Sn and Sn based composites have received significant attention because of their higher capacity ( $990 \text{ mAh g}^{-1}$  for  $\text{Li}_{4.4}\text{Sn}$ ) and abundant availability in nature.[7, 11] Although the neighbors of Sn in group IV, *i.e.*, Si and Ge, are also well known for their extraordinary theoretical capacities ( $4200 \text{ mAh g}^{-1}$  for  $\text{Li}_{4.4}\text{Si}$  and  $1600 \text{ mAh g}^{-1}$  for  $\text{Li}_{4.4}\text{Ge}$ ),[7, 11] but several studies reveal that Sn would be a better choice because of following reasons: (i) Owing to the large interstitial space in Sn, Li diffusion is more favorable in Sn as compared to Si and Ge;[11] (ii) Li-Sn compounds are enthalpically more stable, followed by Li-Ge and Li-Si compounds;[11] (iii) Sn is ductile in nature while Si and Ge are brittle, which makes the mechanical integrity of Sn better than the preceding group IV elements;[13, 14] (iv) Being a metal, electrical conductivity of Sn is better than Si and Ge,[15] *etc.* Besides having several advantages, the application of Sn as an anode is still far from commercialization because of huge irreversible capacity loss, particle fracture, and electrochemical pulverization due to drastic variation in volume during lithiation-delithiation process ( $\sim 257\%$ ). [8, 10, 11, 16] The microscopic mechanisms underlying these phenomena are still not entirely understood. Thus, in order to gain a deep insight into the failure mechanism of a Li-Sn battery during charging and discharging, and to find a possible way to improve its mechanical properties, it is required to understand the process at the atomistic level. This can be done by studying the variation in the atomic structure and properties of Sn anode (“fingerprint”) during lithiation process, in detail.

The Li-Sn binary system has a very rich phase diagram. In an increasing order of lithium content, the following phases are experimentally reported:  $\text{Li}_2\text{Sn}_5$  ( $\text{P4}/\text{mbm}$ ,  $Z = 2$ ), [17–19]  $\text{Li}_1\text{Sn}_1$  {( $\text{P2}/\text{m}$ ,  $Z = 3$ ), ( $\text{I4}_1/\text{amd}$ ,  $Z = 12$ )}, [17, 18, 20, 21]  $\text{Li}_7\text{Sn}_3$  ( $\text{P2}_1/\text{m}$ ,  $Z = 2$ ), [17, 18, 22]  $\text{Li}_5\text{Sn}_2$  ( $\text{R}\bar{3}\text{m}$ ,  $Z = 2$ ), [17, 18, 23]  $\text{Li}_{13}\text{Sn}_5$  ( $\text{P}\bar{3}\text{m1}$ ,  $Z = 1$ ), [17, 18, 24]  $\text{Li}_7\text{Sn}_2$  ( $\text{Cmmm}$ ,  $Z = 2$ ), [17, 18, 25]  $\text{Li}_{17}\text{Sn}_4$  ( $\text{F}\bar{4}3\text{m}$ ,  $Z = 20$ ). [17, 18, 26, 27] The crystal structure of the most lithiated phase  $\text{Li}_{17}\text{Sn}_4$ , was previously thought to be of stoichiometry  $\text{Li}_{22}\text{Sn}_5$ , [28] but this has been corrected by Goward et al. and Lupu et al [26, 27] in the beginning of this century. The current phase diagram of Li-Sn systems has been made at atmospheric pressure and high temperature and there still lies a large uncertainty in the Li-rich part of Li-Sn phase diagram at high pressure. While, it has already been demonstrated that the structure and properties of both end members of Li-Sn systems can largely be modified with the use of pressure.[29, 30] Thus, pressure can be used as an extra variable for engineering the structure and properties of Li-Sn compounds. Apart from this, there remains other significant advantages to study the Li-Sn phase diagram at moderately high pressure for high performance LIBs, such as: (i) Pressure can significantly diminish the melting point of materials and enrich the structural chemistry of compounds. Under pressure many unusual stoichiometric which are basically impossible at ambient pressure, can be synthesized with very exotic chemical behavior,[31–33] which may even survive the decompression from high to ambient pressure; (ii) High pressure phases when quenched at ambient pressure, often possess superior mechanical properties; [16] (iii) Quenched high pressure phases can directly be used as pre-lithiated anode materials for void space manipulation during lithiation-delithiation process and hence, for providing the better performance of anode in LIBs.[34, 35]

In past few years, with the evolution of powerful computational algorithms and methods such as evolutionary algorithm, random sampling, minima hopping etc., stable structures of several unknown and novel materials at ambient and high pressure conditions have been discovered, which have also been later confirmed by experiments.[36–40] Very recently, such studies have been performed for studying Li-Si and Li-Ge compounds at ambient conditions.[41–43] These studies confirmed the existence of experimentally reported phases of the system, and at the same time enriched the phase diagram of both Li-Si and Li-Ge with the discovery of several new stable and metastable structures. Furthermore, Zeng et al.[16] predicted and synthesized a new phase of  $\text{Li}_{15}\text{Si}_4$  ( $\beta$ -phase) at 7 GPa, while very recently,

Zhang et al.[33] also revealed the possibility of existence of several Li-rich Li-Si compounds at high pressure. However, to the best of our knowledge, no such study has been done to date on the Li-Sn system, which is one of the potential candidate for the LIBs. Therefore, in current work, we aim to investigate the Li-Sn binary phase diagram at ambient and moderate high pressure (up to 20 GPa) by performing an extensive search on the Li-Sn systems using the evolutionary algorithm code USPEX, in conjunction with first-principles density functional theory (DFT) based calculations.[36–38] Besides the experimentally reported well known structures, our study reveals several new stable and metastable compounds of Li-Sn with quite diverse and unusual crystal structures. This includes prediction of one of the most stable compound, i.e.,  $\text{Li}_8\text{Sn}_3$  at ambient pressure, and several Li-rich metastable and stable phases at ambient and high pressure, respectively. It is noteworthy to mention that possibly not all but several low-energy metastable compound can be synthesized and they can exhibit superior properties than their corresponding stable phases.[44, 45] Furthermore, in our quest for a better understanding of the Li-Sn cell mechanism, we have also calculated electrochemical, mechanical, and electronic properties of all stable and metastable Li-Sn compounds. We believe that our study will provide a basis for future experimental work.

## II. METHODS

We used evolutionary algorithm based technique as implemented in the USPEX code,[36–38] together with DFT to find stable and metastable Li – Sn compounds as well as their ground state structures, at ambient and high pressure. USPEX has already been demonstrated as a powerful tool to determine the lowest energy structure *via* global minimization of the surface free-energy, with great success.[16, 31] Our calculations to search for stable and metastable structures of Li-Sn compounds were carried out using USPEX in two steps. Firstly, most promising compositions of Li – Sn compounds were explored through variable composition method at 1 atm, 5, 10, and 20 GPa pressure considering up to 40 atoms per unit cell. The calculations were carried out over the course of 50-60 generations where, the first generation was blossomed randomly with 150-200 structures by sampling 20-25 different compositions. For the subsequent generations, 40 child structures were produced, through different symmetry generators, namely heredity, transmutation, softmutation, and random, with probabilities of 40%, 20%, 20%, and 20%, respectively. In second step, a fixed composition search of each ambiguous stoichiometry of Li – Sn compounds with different number of “cell formula” units (depending upon the stoichiometry, it varies from 1 to 5) was carried out for over 30-40 generations, with 30-35 different structures in each generation. The population of first generation in fixed composition search was also set with 80-120 structures, in order to densely map the configuration space of random search. Negative enthalpy of formation which is the basic criterion for finding the energetically stable compounds was calculated *via* below equation:

$$\Delta H_f(\text{Li}_x\text{Sn}_y) = \frac{[\text{H}(\text{Li}_x\text{Sn}_y) - x\text{H}(\text{Li}) - y\text{H}(\text{Sn})]}{(x + y)} \quad (1)$$

where,  $H = U + PV$  is the enthalpy of each compositions in their crystal form and  $\Delta H_f$  is the formation enthalpy of the compound per atom. In the expression of enthalpy,  $U$ ,  $P$ , and  $V$  represent the internal energy, pressure, and volume, respectively.

It should be noted that for a given stoichiometry and pressure, the structure having lowest negative value of formation enthalpy can be considered as most favorable phase as compared to others. But, in order to judge the thermodynamic stability of a particular Li – Sn compound with respect to two nearest neighbor compositions and/or pure elements at ambient or high pressure, it is important to draw the thermodynamics convex hull. The thermodynamics convex hull which, is a representater of compound’s formation enthalpy with its respective stoichiometric ratio at given pressure, is also able to elucidate the all possible decomposition routes. Basically, a phase can be identified as thermodynamically stable ground state phase if it lies on the convex hull. Hence, the stoichiometries that do not have a representative structure on the convex hull, are considered as either metastable or unstable. However, in order to govern the local (meta)stability, we further investigated the phonon dispersion curves of all respective Li – Sn compounds. A structure can be considered as dynamically stable, if and only if, no imaginary phonon frequencies are detected through out the Brillouin zone in phonon dispersion curve. In principle, a metastable compound can also be synthesized.[44, 45]

The structure relaxation of all compositions generated by USPEX were accomplished using first-principles density functional theory (DFT) as implemented in the Vienna Ab-initio Simulation Package (VASP).[46, 47] A plane-wave basis set was employed to expand the valence electronic wave functions, while the projector augmented-wave (PAW) type pseudo-potentials were considered to account the interactions with nuclei and core electrons.[48] For electron-electron exchange and correlation interactions, the functional of Perdew-Burke-Ernzerhof (PBE), a form of the generalized gradient approximation (GGA) was used, in the current work.[49] The plane-wave kinetic energy cutoff was considered

as 700 eV, while the reciprocal space resolution for  $k$ -points generation in final structures relaxation and enthalpy calculations was set to  $0.02 \times 2\pi \text{ \AA}^{-1}$  with uniform  $\Gamma$ -centered meshes. All the above mentioned parameters ensure that the enthalpy calculations are well converged with fluctuation in enthalpy to be less than 1 meV/atom. In order to probe the dynamical stability, phonon frequencies throughout the whole Brillouin Zone were calculated using density functional perturbation theory (DFPT) as implemented in the VASP code along with the Phonopy package.[50] Depending upon the primitive cells structure,  $l \times m \times n$  supercells (where,  $2 \leq l, m, n \leq 3$ ) were used to calculate the phonon dispersion curve.

In order to analyse electrochemical properties of Li-Sn compounds with lithiation at different pressure value, we calculated the Li-insertion voltage. For this, we considered only the stable compositions of Li-Sn that lie on the convex hull tie line at a given pressure, and assumed that the reaction proceeds from pure Sn to subsequent Li-rich phases by exchange of Li atoms only. Therefore, for a general reaction  $\text{Li}_{x_0}\text{Sn} + (x_1 - x_0)\text{Li} \rightarrow \text{Li}_{x_1}\text{Sn}$ , the cell voltage between these two compositions was computed using a well-established formula:[51]

$$V = \frac{G(\text{Li}_{x_1}\text{Sn}) - G(\text{Li}_{x_0}\text{Sn}) - (x_1 - x_0)G(\text{Li})}{(x_1 - x_0)} \quad (2)$$

where,  $G(\text{Li}_x\text{Sn})$  and  $G(\text{Li})$  are the Gibbs free energy of  $\text{Li}_x\text{Sn}$  per Sn atom and the Gibbs free energy of Li per Li atom, respectively. Here, we neglected the contribution of zero-point energy and lattice vibrational energy to the Gibbs free energy as it is relatively very small and further reduces when used in the above formula. Thus, we approximated  $G$  with the enthalpy of each composition.

In addition, the theoretical gravimetric capacity, GC, was also determined using following equation:

$$\text{GC} = \frac{xF}{M_{\text{Sn}}} \quad (3)$$

where,  $x$  is the number of Li atoms present in  $\text{Li}_x\text{Sn}$ ,  $F$  is the Faraday constant, and  $M_{\text{Sn}}$  represents the Molar-Mass of Sn.

To examine mechanical properties, elastic constants were calculated using the VASP code, while the bulk modulus ( $B$ ), shear modulus ( $G$ ), Young modulus ( $Y$ ), and Poisson's ratio ( $\nu$ ) were estimated using the Voigt-Reuss-Hill approximation (Section 12 of SI).[52]

### III. RESULTS AND DISCUSSIONS

#### A. Thermodynamic Stability and Phase Diagram of Li – Sn Compounds.

To explore the stable and metastable Li-Sn compounds in the pressure ranging from 1 atm to 20 GPa, we computed convex hull and pressure-composition phase diagram, depicted in Fig.1. It can be noted from the phase diagram (Fig.1-(b)) that within the given pressure range, Li exhibits two different stable phases:  $\text{Im}\bar{3}\text{m}$  (1 atm–7.6 GPa) and  $\text{Fm}\bar{3}\text{m}$  (7.6 GPa–20 GPa), while Sn possesses three stable phases viz.  $\text{Fd}\bar{3}\text{m}$  (1 atm–0.8 GPa),  $\text{I4}_1/\text{amd}$  (0.8 GPa–7.2 GPa), and  $\text{I4}/\text{mmm}$  (7.2 GPa–20 GPa). This phase sequence for pure Li and Sn are also in accordance with the previous experimental and theoretical data.[53–56] In order to draw the thermodynamic convex hull at different pressure, enthalpy of appropriate phase of pure Li and Sn are considered. Here, it should also be noted that in our calculations we considered maximum of 40 atoms per unit cell. This restricts us to obtain the stoichiometry  $\text{Li}_{17}\text{Sn}_4$  ( $\text{F}\bar{4}3\text{m}$ ,  $Z = 20$ ) in our search as  $\text{Li}_{17}\text{Sn}_4$  contains 420 atoms in the conventional cell, which are beyond our limit to consider. However, in order to account the effect of  $\text{Li}_{17}\text{Sn}_4$  on the thermodynamical stability of other compounds, we explicitly considered the formation enthalpy of  $\text{Li}_{17}\text{Sn}_4$  (calculated separately) to draw convex hull at the pressure values of 1 atm, 5, 10, and 20 GPa. In figure showing convex hull (Fig.1(a)), thermodynamically stable phases of Li-Sn (except  $\text{Li}_{17}\text{Sn}_4$ ) are represented with blue circles, while red squares are used to identify the low-lying local minima on all the convex hull. Meanwhile, the same is represented by green circle and yellow square, respectively, for the  $\text{Li}_{17}\text{Sn}_4$ .

On analysing the convex hull for 1 atm pressure (Fig.1(a)&(b)), we found that our *ab initio* evolutionary search correctly predicts most of the experimentally known Li-Sn compositions and their respective phases, except for  $\text{Li}_7\text{Sn}_2$ . In case of  $\text{Li}_7\text{Sn}_2$  experimentally known phase is  $\text{Cmmm}$ , while we found  $\text{P}\bar{3}\text{m}1$  phase to be more stable than  $\text{Cmmm}$ . However, the difference in the enthalpy for both phases is just 6 meV/atoms, which is in agreement with results of Geneser et al.[57] From our calculations, the experimentally known stoichiometries(phases) such as  $\text{Li}_1\text{Sn}_1$  ( $\text{P2}/\text{m}$ ),  $\text{Li}_{13}\text{Sn}_5$  ( $\text{P}\bar{3}\text{m}1$ ),  $\text{Li}_8\text{Sn}_3$  ( $\text{R}\bar{3}\text{m}$ ),  $\text{Li}_7\text{Sn}_2$  ( $\text{P}\bar{3}\text{m}1$ ), and  $\text{Li}_{17}\text{Sn}_4$  ( $\text{F}\bar{4}3\text{m}$ ), are found to lie on convex-hull tie-line, while

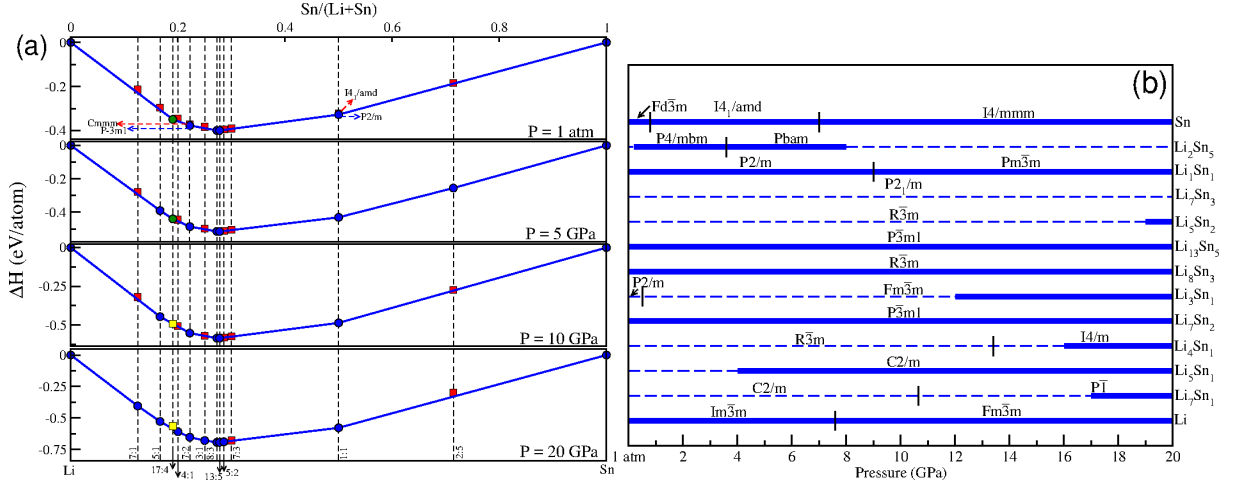


Figure 1. (a) Convex hull for the Li-Sn system at 1 atm, 5, 10, and 20 GPa pressure. Thermodynamically stable phases of Li-Sn (except  $\text{Li}_{17}\text{Sn}_4$ ) are represented with blue circles, while red squares are used to identify the low-energy metastable phases. Meanwhile, the same is represented by green circle and yellow square, respectively, for the  $\text{Li}_{17}\text{Sn}_4$ . (b) Pressure-composition phase diagram of the Li-Sn system ranging from 1 atm to 20 GPa. The stable and metastable phases are shown by solid bold and thin dash lines, respectively.

the other experimentally known stoichiometries like  $\text{Li}_2\text{Sn}_5$  ( $\text{P4}/\text{mbm}$ ),  $\text{Li}_7\text{Sn}_3$  ( $\text{P2}_1/\text{m}$ ), and  $\text{Li}_5\text{Sn}_2$  ( $\text{R}\bar{3}\text{m}$ ) are found marginally above the convex-hull tie-line ( $\sim 1 - 3$  meV/atom), representing these phases to be metastable at 1 atm pressure, as none of the structures possess dynamical anharmonicity in their respective phonon dispersion curves (Fig. S1 in SI). The decomposition energy of these experimentally identified compounds in terms of measured vertical length from the convex hull are tabulated in Table T1 of SI. Finally, in order to give a firm insight in our theoretical findings and to cross check the thermodynamics stability of experimentally reported Li-Sn compounds, we compared our results with the convex hull build upon the experimental structures available in open quantum material database (OQMD).[58, 59] Except for  $\text{Li}_2\text{Sn}_5$  (after inclusion of formation enthalpy of  $\text{Li}_{17}\text{Sn}_4$  in the convexhull), our results are found to be in good agreement with the OQMD based convex hull. In case of  $\text{Li}_2\text{Sn}_5$ , the decomposition energy is less than 3 meV/atom. This energy difference lies close to the boundary line of numerical accuracy in our calculations. Therefore, we believe that such discrepancy can be ignored.

Besides the above mentioned known compositions in the Li-Sn system, very interestingly, our calculations revealed one of the most stable stoichiometry (next to  $\text{Li}_{13}\text{Sn}_5$ ) of Li-Sn, i.e.,  $\text{Li}_8\text{Sn}_3$  ( $\text{R}\bar{3}\text{m}$ ) which currently does not exist in the phase-diagram for Li-Sn, neither at ambient conditions nor at high temperature or pressure. While, our calculations predict this composition to be stable throughout the investigated pressure range. This composition, however, was previously predicted by Gasior et al. in 1996 using electromotive force methods,[60] but its structure and phase was not known until now and thus, this composition is still missing in the Li-Sn phase diagram. But, our results strongly convince us for its existence and thus, we believe that careful measurements at ambient conditions can perhaps discover this composition experimentally as well. Furthermore, our calculations also acknowledge four yet unknown Li-rich compositions:  $\text{Li}_3\text{Sn}_1$  ( $\text{P2}/\text{m}$ ),  $\text{Li}_4\text{Sn}_1$  ( $\text{R}\bar{3}\text{m}$ ),  $\text{Li}_5\text{Sn}_1$  ( $\text{C2}/\text{m}$ ), and  $\text{Li}_7\text{Sn}_1$  ( $\text{C2}/\text{m}$ ). In case of 1 atm pressure, all these stoichiometries do not lie on the convex hull tie-line but the absence of imaginary frequencies in phonon dispersion curves (Fig. S1 in SI) and calculation of mechanical properties (which we will discuss in later section), disclose these compounds to be metastable at 1 atm pressure. Moreover, not to ignore the crucial role played by ion-dynamics in deciding the ground state energy of materials, especially of light materials, we re-calculated the formation enthalpies at 1 atm pressure by considering the vibrational contributions (zero-point energy). The results presented in Table T2 of SI, clearly indicate the negligible effect of zero-point energy (ZPE) on the formation enthalpies for all Li-Sn compounds ( $\sim$ smaller by three orders of magnitude), which is not even changing the order of stability of the compounds. We therefore have neglected the contribution of ZPE while addressing the relative stability of Li-Sn compounds at higher pressure. It should be noted that since the metastable compounds, especially the low-energy ones, are synthesizable under certain thermodynamical conditions,[44, 45] we believe that most of above discussed Li-rich compositions can be synthesized. Moreover, if synthesized, these metastable/stable compounds should be recoverable as well, when decompressed to ambient pressure, again because of non-existence of negative frequencies in their phonon spectra at 1 atm.[61] Also, one can not exclude the possibility of formation of these phases during lithiation of Sn anode since at the end of the discharge of the Sb/Na cell Darwiche et al.[62] observed the presence of cubic  $\text{Na}_3\text{Sb}$ , which is metastable at ambient pressure and can only be synthesized under high pressure. Thus, a careful experimental study



is indeed needed to focus on the formation of metastable phases during lithiation-delithiation.

To study the effect of high pressure ( $1\text{ atm} \leq P \leq 20\text{ GPa}$ ), we computed the convex-hull at 5, 10, and 20 GPa. It can be clearly noticed from the Fig.1(a) that at 5 and 10 GPa pressure, except  $\text{Li}_2\text{Sn}_5$  and  $\text{Li}_5\text{Sn}_1$ , all other stoichiometries show similar stability as in case of 1 atm pressure. Our calculations reveal  $\text{Li}_2\text{Sn}_5$  to be thermodynamically stable between pressure range 0.2 GPa–8 GPa, while  $\text{Li}_5\text{Sn}_1$  is found to be stable from 4 GPa onwards. Additionally, a pressure induced phase transformation is also observed in the stoichiometry  $\text{Li}_2\text{Sn}_5$  and  $\text{Li}_1\text{Sn}_1$ . In case of  $\text{Li}_2\text{Sn}_5$ , the  $\text{P4}/\text{mbm}$  phase gets transformed to  $\text{Pbam}$  above 3.9 GPa, while  $\text{Li}_1\text{Sn}_1$  transforms from  $\text{P2}/\text{m}$  to  $\text{Pm}\bar{3}\text{m}$  at around 9 GPa, which is also in agreement with the study of Genser et al.[57] Also, it is found that the experimentally most lithiated phase,  $\text{Li}_{17}\text{Sn}_4$ , losses its thermodynamic stability at around 9.8 GPa. Above this pressure,  $\text{Li}_{17}\text{Sn}_4$  shall decompose into  $\text{Li}_5\text{Sn}_1$  ( $\text{C2}/\text{m}$ ) and  $\text{Li}_7\text{Sn}_2$  ( $\text{P}\bar{3}\text{m1}$ ) (i.e.,  $\text{Li}_{17}\text{Sn}_4(\text{F}\bar{4}3\text{m}) \xrightarrow{9.8\text{ GPa}} \text{Li}_5\text{Sn}_1(\text{C2}/\text{m}) + \text{Li}_7\text{Sn}_2(\text{P}\bar{3}\text{m1})$ ), as shown in Fig. S3 in SI. The most fascinating results are observed at 20 GPa pressure. Our calculations disclose a diverse chemistry of Li-Sn compounds by predicting the stability of some novel exotic Li-rich Li-Sn compounds. Except for  $\text{Li}_2\text{Sn}_5$  and  $\text{Li}_7\text{Sn}_3$ , all metastable stoichiometries such as  $\text{Li}_5\text{Sn}_2$ ,  $\text{Li}_3\text{Sn}_1$ ,  $\text{Li}_4\text{Sn}_1$ , and  $\text{Li}_7\text{Sn}_1$  become stable at this range of pressure. Moreover, it should be noted here that the compositions:  $\text{Li}_5\text{Sn}_1$  and  $\text{Li}_7\text{Sn}_1$ , can accommodate more lithium as compared to the presently known highest lithiated compound,  $\text{Li}_{17}\text{Sn}_4$ . Though it is understandable from the perspective of LIBs, that the pressure range where these Li-rich compounds get stable is quite high, but not to forget that these Li-rich compounds should be recoverable when quenched to ambient pressure, as discussed above.

The phase diagram of Li-Sn compounds presented in Fig.1(b) provides a clear picture of different phases acquired by individual composition in the pressure range of 1 atm to 20 GPa. Among several investigated Li-Sn compositions, robust stability and no phase transition are observed in three of the compounds, i.e.,  $\text{Li}_{13}\text{Sn}_5$ ,  $\text{Li}_8\text{Sn}_3$ , and  $\text{Li}_7\text{Sn}_2$ . Through out the investigated pressure range (1 atm–20 GPa) they exhibit  $\text{P}\bar{3}\text{m1}$ ,  $\text{R}\bar{3}\text{m}$ , and  $\text{P}\bar{3}\text{m1}$  space group symmetry, respectively. Interestingly,  $\text{Li}_{13}\text{Sn}_5$  and  $\text{Li}_8\text{Sn}_3$  are also identified as the most stable Li-Sn compounds (Fig.1(a)). Other than these,  $\text{Li}_7\text{Sn}_3$ ,  $\text{Li}_5\text{Sn}_2$ , and  $\text{Li}_5\text{Sn}_1$  are also found to remain in a single space group symmetry viz.  $\text{P2}_1/\text{m}$ ,  $\text{R}\bar{3}\text{m}$ , and  $\text{C2}/\text{m}$ , respectively, in the entire pressure range. However, like former compositions ( $\text{Li}_{13}\text{Sn}_5$ ,  $\text{Li}_8\text{Sn}_3$ , and  $\text{Li}_7\text{Sn}_2$ ), these materials ( $\text{Li}_7\text{Sn}_3$ ,  $\text{Li}_5\text{Sn}_2$ , and  $\text{Li}_5\text{Sn}_1$ ) are not found to be stable through out the investigated pressure range. Our calculations reveal  $\text{Li}_7\text{Sn}_3$  to be metastable in the given pressure range, while  $\text{Li}_5\text{Sn}_2$  and  $\text{Li}_5\text{Sn}_1$  get stable above 18.2 and 4 GPa, respectively. Other novel stoichiometries like  $\text{Li}_3\text{Sn}_1$ ,  $\text{Li}_4\text{Sn}_1$ , and  $\text{Li}_7\text{Sn}_1$  are found to be stable at 12, 16, and 17 GPa, respectively. These compounds are also found to change phase from  $\text{P2}/\text{m}$  to  $\text{Fm}\bar{3}\text{m}$  at 0.8 GPa,  $\text{R}\bar{3}\text{m}$  to  $\text{I4}/\text{m}$  at 13.2 GPa, and  $\text{C2}/\text{m}$  to  $\text{P}\bar{1}$  at 10.8 GPa, respectively (Fig.1(b)).

## B. Crystal Structure of Li – Sn Compounds

In Table I, lattice parameters for each of the stable and metastable Li-Sn compounds identified by our calculations at 1 atm, 5, 10, and 20 GPa are tabulated. At 1 atm pressure, except for  $\text{Li}_7\text{Sn}_2$ , the structural information predicted by our calculations for the experimentally known stoichiometries like  $\text{Li}_2\text{Sn}_5$ ,  $\text{Li}_1\text{Sn}_1$ ,  $\text{Li}_7\text{Sn}_3$ ,  $\text{Li}_5\text{Sn}_2$ , and  $\text{Li}_{13}\text{Sn}_5$  are found to be in very good agreement with experimental results. Our calculations also predicted the unknown structure of once predicted stoichiometries like  $\text{Li}_8\text{Sn}_3$ , [60]  $\text{Li}_3\text{Sn}_1$ , [63] and  $\text{Li}_4\text{Sn}_1$ , [64] together with the structure of novel Li-rich compounds:  $\text{Li}_5\text{Sn}_1$  and  $\text{Li}_7\text{Sn}_1$ . The structure of already known Li-Sn stoichiometries are discussed in detail in Section 5 of SI. While, here, we only discuss the structure of all yet unexplored Li-Sn stoichiometries, predicted by our calculations as metastable or stable chemical compositions of Li-Sn in the pressure range of 1 atm–20 GPa. The crystallographic details of each of these structures are given in Table T12 of SI.

### 1. Unknown Structures of Already Predicted Li-Sn Compounds

**$\text{Li}_8\text{Sn}_3$ :** In 1996, Gasior et al.[60] revealed a possible existence of a new stoichiometry  $\text{Li}_8\text{Sn}_3$  along with the seven previously reported compounds when they studied the Li–Sn system by means of electromotive force (EMF) method at the composition range of 2.4–95.2 at% of Li. However, to the best of our knowledge the crystal structure of that newly predicted phase is yet unknown and our calculations predict its structure for the first time. We predicted  $\text{Li}_8\text{Sn}_3$  to be one of the most stable Li-Sn compound (also at 1 atm pressure) and identify it to crystallize in trigonal crystal system with  $\text{R}\bar{3}\text{m}$  ( $Z=3$ ) space group symmetry with  $a = 4.684\text{ \AA}$  and  $c = 31.582\text{ \AA}$  at ambient pressure (Fig.2(i) and Table I). Interestingly, the structure of  $\text{Li}_8\text{Sn}_3$  is isostructure with  $\text{Li}_8\text{Ge}_3$  [42] and high pressure  $\text{Li}_8\text{C}_3$  structure.[65] All these compounds have Li as cation and anion belonging to group IV element of periodic table, thus, should have similar structure. This gives us confidence about correctness of our predicted structure. On investigating the structure in detail, we found that the arrangement of atoms in  $\text{Li}_8\text{Sn}_3$  is very similar to  $\text{Li}_{13}\text{Sn}_5$  structure. The only difference is

Table I. The space group and calculated equilibrium lattice parameters  $a$  (Å),  $b$  (Å), and  $c$  (Å),  $\alpha$ (deg),  $\beta$ (deg),  $\gamma$ (deg), and volume ( $\text{\AA}^3/\text{atom}$ ) at given pressure for Li, Sn and Li-Sn compounds are given. Gravimetric capacities of corresponding Li-Sn compounds are written insight.

System (G/C)	Pressure	Space	a	b	c	$\alpha$	$\beta$	$\gamma$	Volume	System (G/C)	Pressure	Space	a	b	c	$\alpha$	$\beta$	$\gamma$	Volume
(mAh/g)		Group (f.u)	(Å)	(Å)	(Å)	(°)	(°)	(°)	(Å <sup>3</sup> /atom)	(mAh/g)		Group (f.u)	(Å)	(Å)	(Å)	(°)	(°)	(°)	(Å <sup>3</sup> /atom)
Sn (-)	1 atm	Fd3m(Z=8)	6.651	6.651	6.651	90.00	90.00	90.00	36.78	Li (-)	1 atm	Im3m(Z=2)	3.439	3.439	3.439	90.00	90.00	90.00	20.33
	5 GPa	I4 <sub>1</sub> /amd(Z=4)	5.948	5.948	3.201	90.00	90.00	90.00	28.31		5 GPa	Im3m(Z=2)	3.175	3.175	3.175	90.00	90.00	90.00	16.00
	10 GPa	I4/mmm(Z=2)	3.778	3.778	3.349	90.00	90.00	90.00	23.91		10 GPa	Fm3m(Z=4)	3.814	3.814	3.814	90.00	90.00	90.00	13.87
	20 GPa	I4/mmm(Z=2)	3.647	3.647	3.285	90.00	90.00	90.00	21.84		20 GPa	Fm3m(Z=4)	3.591	3.591	3.591	90.00	90.00	90.00	11.57
Li <sub>2</sub> Sn <sub>5</sub> (90)	1 atm	P4/mbm(Z=2)	10.378	10.378	3.141	90.00	90.00	90.00	24.17	Li <sub>7</sub> Sn <sub>1</sub> (1580)	1 atm	C2/m(Z=4)	15.678	4.826	8.058	90.00	102.67	90.00	18.59
	5 GPa	Pbam(Z=2)	10.365	9.745	3.045	90.00	90.00	90.00	21.97		5 GPa	C2/m(Z=4)	14.762	4.556	7.598	90.00	102.40	90.00	15.60
	10 GPa	Pbam(Z=2)	10.247	9.407	2.981	90.00	90.00	90.00	20.52		10 GPa	C2/m(Z=4)	14.208	4.392	7.324	90.00	102.14	90.00	13.96
	20 GPa	Pbam(Z=2)	10.090	8.955	2.885	90.00	90.00	90.00	18.62		20 GPa	P $\bar{1}$ (Z=2)	4.609	6.693	6.697	67.57	79.92	80.25	11.68
Li <sub>13</sub> Sn <sub>1</sub> (226)	1 atm	P2/m(Z=3)	5.178	3.225	7.812	90.00	105.25	90.00	20.98	Li <sub>5</sub> Sn <sub>1</sub> (1129)	1 atm	C2/m(Z=8)	15.918	5.738	12.043	90.00	128.86	90.00	17.84
	5 GPa	P2/m(Z=3)	4.940	3.145	7.526	90.00	106.18	90.00	18.72		5 GPa	C2/m(Z=8)	15.135	5.474	11.453	90.00	128.87	90.00	15.39
	10 GPa	Pm3m(Z=1)	3.248	3.248	3.248	90.00	90.00	90.00	17.14		10 GPa	C2/m(Z=8)	14.631	5.308	11.076	90.00	128.83	90.00	13.96
	20 GPa	Pm3m(Z=1)	3.135	3.135	3.135	90.00	90.00	90.00	15.41		20 GPa	C2/m(Z=8)	13.948	5.089	10.568	90.00	128.71	90.00	12.20
Li <sub>7</sub> Sn <sub>3</sub> (527)	1 atm	P2 <sub>1</sub> /m(Z=2)	8.562	4.738	9.491	90.00	106.10	90.00	18.50	Li <sub>17</sub> Sn <sub>4</sub> (960)	1 atm	F43m(Z=20)	19.714	19.714	19.714	90.00	90.00	90.00	18.24
	5 GPa	P2 <sub>1</sub> /m(Z=2)	8.225	4.528	9.092	90.00	106.07	90.00	16.27		5 GPa	F43m(Z=20)	18.789	18.789	18.789	90.00	90.00	90.00	15.79
	10 GPa	P2 <sub>1</sub> /m(Z=2)	8.009	4.387	8.341	90.00	106.05	90.00	14.91		10 GPa	F43m(Z=20)	18.198	18.198	18.198	90.00	90.00	90.00	14.35
	20 GPa	P2 <sub>1</sub> /m(Z=2)	7.710	4.196	8.489	90.00	106.03	90.00	13.20		20 GPa	F43m(Z=20)	17.398	17.398	17.398	90.00	90.00	90.00	12.54
Li <sub>5</sub> Sn <sub>2</sub> (564)	1 atm	R3m(Z=3)	4.732	4.732	19.810	90.00	90.00	120.00	18.29	Li <sub>4</sub> Sn <sub>1</sub> (903)	1 atm	R3m(Z=3)	4.742	4.742	13.932	90.00	90.00	120.00	18.08
	5 GPa	R3m(Z=3)	4.520	4.520	19.079	90.00	90.00	120.00	16.07		5 GPa	R3m(Z=3)	4.524	4.524	13.173	90.00	90.00	120.00	15.57
	10 GPa	R3m(Z=3)	4.376	4.376	18.629	90.00	90.00	120.00	14.72		10 GPa	R3m(Z=3)	4.386	4.386	12.701	90.00	90.00	120.00	14.11
	20 GPa	R3m(Z=3)	4.187	4.187	17.994	90.00	90.00	120.00	13.01		20 GPa	I4/m(Z=10)	11.965	11.965	4.241	90.00	90.00	90.00	12.14
Li <sub>13</sub> Sn <sub>5</sub> (587)	1 atm	P3m1(Z=1)	4.702	4.702	17.133	90.00	90.00	120.00	18.23	Li <sub>7</sub> Sn <sub>2</sub> (790)	1 atm	P3m1(Z=1)	4.681	4.681	8.501	90.00	90.00	120.00	17.93
	5 GPa	P3m1(Z=1)	4.495	4.495	16.458	90.00	90.00	120.00	16.00		5 GPa	P3m1(Z=1)	4.476	4.476	8.088	90.00	90.00	120.00	15.59
	10 GPa	P3m1(Z=1)	4.358	4.358	16.020	90.00	90.00	120.00	14.64		10 GPa	P3m1(Z=1)	4.341	4.341	7.828	90.00	90.00	120.00	14.20
	20 GPa	P3m1(Z=1)	4.173	4.173	15.433	90.00	90.00	120.00	12.93		20 GPa	P3m1(Z=1)	4.160	4.160	7.485	90.00	90.00	120.00	12.46
Li <sub>8</sub> Sn <sub>3</sub> (602)	1 atm	R3m(Z=3)	4.684	4.684	31.582	90.00	90.00	120.00	18.18	Li <sub>3</sub> Sn <sub>1</sub> (677)	1 atm	P2/m(Z=3)	6.885	4.623	7.060	90.00	104.07	90.00	18.16
	5 GPa	R3m(Z=3)	4.478	4.478	30.298	90.00	90.00	120.00	15.94		5 GPa	Fm3m(Z=4)	6.305	6.305	6.305	90.00	90.00	90.00	15.67
	10 GPa	R3m(Z=3)	4.343	4.343	29.462	90.00	90.00	120.00	14.58		10 GPa	Fm3m(Z=4)	6.119	6.119	6.119	90.00	90.00	90.00	14.32
	20 GPa	R3m(Z=3)	4.161	4.161	28.337	90.00	90.00	120.00	12.87		20 GPa	Fm3m(Z=4)	5.867	5.867	5.867	90.00	90.00	90.00	12.62

that dimers and monomers of Sn repeat after every 4 Li atoms instead of 5 Li atoms in case of Li<sub>13</sub>Sn<sub>5</sub> structure. The dumbbell length of Sn atoms ( $\sim 2.91$  Å) however remains same as in Li<sub>5</sub>Sn<sub>2</sub> and Li<sub>13</sub>Sn<sub>5</sub> structures. With pressure the Li-Li, Li-Sn, and Sn-Sn distance changes from 2.80 Å, 2.80 Å, and 2.91 Å at 1 atm pressure to 2.47 Å, 2.51 Å, and 2.76 Å, respectively, at 20 GPa (Fig. S12 and Table T11 in SI).

**Li<sub>3</sub>Sn<sub>1</sub>:** More than a decade ago, Thackeray et. al.[63] predicted existence of f.c.c.-Li<sub>3</sub>Sn<sub>1</sub> in the intermediate step of lithiation in Sn anode on the basis of argument that it is the basic building block of the experimentally known highest lithiated phase of Sn, i.e., Li<sub>4.4</sub>Sn[28] (corrected stoichiometry is Li<sub>4.25</sub>Sn[26, 27]). They proposed that the transition from Li<sub>3</sub>Sn<sub>1</sub> to Li<sub>4.4</sub>Sn can be stabilized by a small amount of residual copper which helps them to crystallize in f.c.c. structure. Interestingly, our calculations also predicted Li<sub>3</sub>Sn<sub>1</sub> to be thermodynamically stable above 12 GPa pressure, where it crystallizes in Fm3m (f.c.c.) structure with four formula unit (i.e., Z=4) and lattice parameter as  $a = 5.867$  Å at 20 GPa. The structure is isostructural to Li<sub>3</sub>Pb<sub>1</sub> structure, which exist as a stable compound in the Li-Pb phase diagram.[66] Fm3m-Li<sub>3</sub>Sn<sub>1</sub> crystal compromises of “...ABAB...” planner stacking along any of its crystallographic axis (Fig.2(iii)). Under this arrangement the formation of the structure can be interpreted by considering each “A” plane consisting of pure Li atoms and then the subsequent first neighbour planes (i.e., B plane) exhibit both Li and Sn atoms which are arranged in the plane in alternative manner. However, it should be noted here that at ambient pressure (and 0 K temperature), our evolutionary structure search predicts a distorted f.c.c. structure (Fig.2(ii)), space group P2/m, Z = 3 with  $a = 6.885$  Å,  $b = 4.623$  Å,  $c = 7.060$  Å and  $\beta = 104.07^\circ$ ) to be energetically more favorable than the Fm3m - Li<sub>3</sub>Sn<sub>1</sub> (which though transforms into latter structure above 0.5 GPa pressure (Fig.S7(a) in SI)), and this leads to a slight discrepancy between our results and prediction made by Thackeray et al.[63] We attribute this discrepancy to the fact that they considered room temperature while our DFT calculations are fundamentally restricted to deal with 0 K temperature only. Still, in order to picturize the exact phase that may (metastably) exist during lithiation of Sn at ambient pressure and temperature, we plotted the Gibbs free energy for both the phases with temperature at 1 atm (Fig.S7(b) in SI). The contribution to free energy at finite temperature comes from both electronic excitations as well as lattice vibrations. But, the contribution of thermal excitation of electrons to free energy is very small and can be neglected without any loss of generality. Therefore, we only calculated the contribution to free energy due to the lattice excitations under quasi-harmonic approximation. On analyzing Fig.S7(b) in SI, phase transition from P2/m to Fm3m structure near the room temperature ( $\geq 311$  K) can clearly be noticed. Thus, in agreement with prediction made by Thackeray et al.,[63] our study affirms the formation

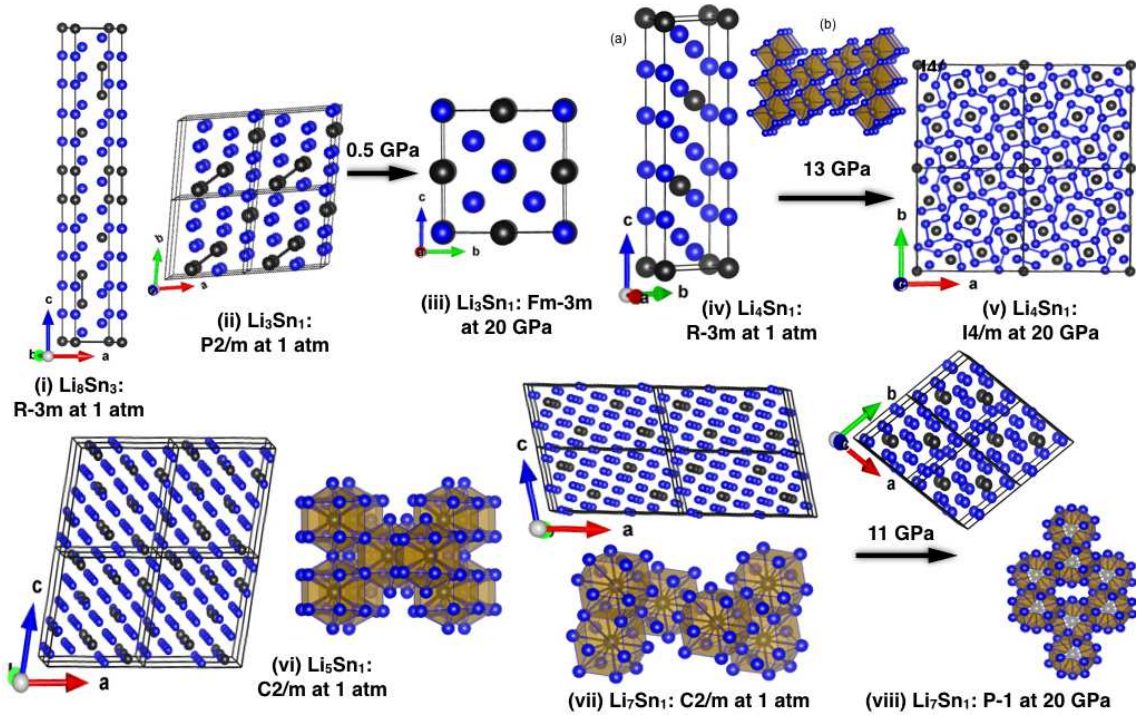


Figure 2. **Crystal structures of the newly predicted Li-Sn compounds.** (i) Crystal structure of  $\text{Li}_8\text{Sn}_3$  ( $\bar{R}3m$ ), (ii & iii) Phase transformation from  $P2/m$  to  $Fm\bar{3}m$  of  $\text{Li}_3\text{Sn}_1$ , (iv-a & v) Phase transformation from  $\bar{R}3m$  to  $I4/m$  of  $\text{Li}_4\text{Sn}_1$ , (iv-b) Polyhedral representation of  $\bar{R}3m$ - $\text{Li}_4\text{Sn}_1$ , (vi) Crystal structure of  $\text{Li}_5\text{Sn}_1$  ( $C2/m$ ) and its corresponding polyhedral representation, and (vii & viii) Phase transformation from  $C2/m$  to  $P\bar{1}$  of  $\text{Li}_7\text{Sn}_1$  and their corresponding polyhedral representation.

of  $Fm\bar{3}m$  -  $\text{Li}_3\text{Sn}_1$  phase during the room temperature lithiation of Sn anode in LIBs. The shortest Li-Li, Li-Sn, and Sn-Sn distance in  $\text{Li}_3\text{Sn}_1$  are found to reduce from 2.77 Å, 2.78 Å, and 2.95 Å in  $P2/m$  phase at 1 atm pressure to 2.55 Å, 2.55 Å, and 4.15 Å, respectively, at 20 GPa in  $Fm\bar{3}m$  phase (Fig. S12 and Table T11 in SI).

**$\text{Li}_4\text{Sn}_1$ :** In mid 80's, Alblas et al.[64] investigated structure of molten Li-Sn alloys using neutron diffraction measurement and discovered a strong short range ordering behavior near  $\text{Li}_4\text{Sn}_1$  composition.[64] Almost same phenomenon was later observed from the extended *ab initio* molecular dynamics (MD) simulations, as well.[57] However, to the best of our knowledge no information about the phase and the structure for the crystalline  $\text{Li}_4\text{Sn}_1$  is yet reported. For the first time, our study reveal two crystalline phases for  $\text{Li}_4\text{Sn}_1$  in the investigated pressure range: trigonal crystal system with space group  $\bar{R}3m$  ( $Z = 3$ , at 1 atm pressure  $a = 4.742$  Å and  $c = 13.932$  Å) between 1 atm–13.4 GPa and tetragonal system with space group  $I4/m$  ( $Z = 10$ ,  $a = 11.965$  and  $c = 4.241$  Å at 20 GPa) from 13.4 GPa to 20 GPa (Fig.1(b)). Though the compound remains metastable till 16 GPa and gets thermodynamically stable only above that but, a structural phase transition from  $\bar{R}3m$  to  $I4/m$  is observed at  $\sim 13$  GPa pressure (Fig.S9 in SI). In  $\bar{R}3m$ - $\text{Li}_4\text{Sn}_1$ , one can notice atomic chains parallel to hexagonal axis (Fig.2(iv)-(a)). Each chain consists of periodic monomers of Sn after every 4 Li atoms. However, in polyhedral representations of the same, (distorted) cubic hexahedron (where length of each side of the distorted cubes is either 3.18 Å or 3.42 Å) with Li atoms at the vertex positions and Sn atoms at the body center positions can be seen in the structure (Fig.2(iv)-(b)). In a cube, each of six Li atoms are connected with three nearby Sn atoms from the adjacent cubes, while each of the other two Li-atoms are connected with one Sn atom within the cube. Thus, the formation of the structure can be interpreted on the basis of extended Zintl–Klemm principle where Sn atoms fulfill the “octet” by acquiring two electrons from six Li-atoms and two more electrons from other two Li-atoms, as expected. On the other hand, the high pressure  $I4/m$  phase compromises “...ABAB...” planner stacking along its crystallographic  $c$ -axis (Fig.2(v)). The atomic layers represented here by A and B are identical and have the same 2D periodicity in the  $ab$  plane, but adjacent layers are displaced relative to each other by  $d_+ = a(\frac{1}{2}, \frac{1}{2}, 0)$ . The shortest Li-Li, Li-Sn, and Sn-Sn distance in  $\bar{R}3m$ - $\text{Li}_3\text{Sn}_1$  phase reduce from 2.60 Å, 2.86 Å, and 4.75 Å at 1 atm pressure to 2.23 Å, 2.48 Å, and 4.19 Å, respectively, at 20 GPa in  $I4/m$  phase (Fig. S12 and Table T11 in SI).



## 2. Newly Discovered Li-Sn Compounds

Experimentally,  $\text{Li}_{17}\text{Sn}_4$  with space group  $F\bar{4}3m$  and  $Z = 20$  is known as the highest lithiated compound of Sn at ambient pressure. However, our *ab initio* evolutionary algorithm search reveals the possible existence of two extremely Li-rich compounds, i.e.,  $\text{Li}_5\text{Sn}_1$  and  $\text{Li}_7\text{Sn}_1$ , at high pressure. Here, the number of Li atoms exceeds the highest formal valence of  $4^-$  for Sn. As a consequence, both the systems are remarkably electron rich. Though at ambient pressure both,  $\text{Li}_5\text{Sn}_1$  and  $\text{Li}_7\text{Sn}_1$  are found metastable but we believe that these stoichiometries might be recovered during the quenching from high pressure to ambient conditions as it does not exhibit modes of negative frequency at ambient pressure (Fig. S1 in SI). If this can be achieved then the Sn anode with higher specific capacity and probably better mechanical properties can be realized.

**$\text{Li}_5\text{Sn}_1$ :** Our calculations predict  $\text{Li}_5\text{Sn}_1$  to crystallize in monoclinic  $C2/m$  phase with  $Z = 8$  through out the investigated pressure range. The lattice parameters at 1 atm pressure are found as:  $a = 15.918 \text{ \AA}$ ,  $b = 5.738 \text{ \AA}$ ,  $c = 12.043 \text{ \AA}$ , and  $\beta = 128.86^\circ$ . The atomic arrangement in  $\text{Li}_5\text{Sn}_1$  can be described as Li sharing 14 fold  $\text{Li}_{14}\text{Sn}$  elongated hexagonal bipyramid with Sn atom located at the center position (Fig.2(vi)). The Li-Sn distance in the cage varies from  $2.88 \text{ \AA}$  -  $3.15 \text{ \AA}$ , while Sn atoms are well separated from each other by distance above  $4.66 \text{ \AA}$  (Fig. S12 and Table T11 in SI). It should also be noted that even at high pressure the Sn atoms remain isolated in  $\text{Li}_5\text{Sn}_1$ .

**$\text{Li}_7\text{Sn}_1$ :** As per our calculations  $\text{Li}_7\text{Sn}_1$  is found to exhibit two possible phases in the pressure range of 1 atm - 20 GPa.  $\text{Li}_7\text{Sn}_1$  first crystallizes in a monoclinic structure with  $C2/m$  symmetry ( $Z = 4$ ,  $a = 15.678 \text{ \AA}$ ,  $b = 4.826 \text{ \AA}$ ,  $c = 8.058 \text{ \AA}$ , and  $\beta = 102.67^\circ$ ) at ambient pressure, and later transforms to triclinic structure with  $P\bar{1}$  symmetry ( $Z = 1$ ,  $a = 4.609 \text{ \AA}$ ,  $b = 6.693 \text{ \AA}$ ,  $c = 6.697 \text{ \AA}$ , and  $\alpha = 67.57^\circ$ ,  $\beta = 79.92^\circ$ ,  $\gamma = 80.25^\circ$  at 20 GPa) above 10.7 GPa (Fig.S10 in SI). Similar to  $\text{Li}_5\text{Sn}_1$ , at 1 atm pressure  $C2/m$  -  $\text{Li}_7\text{Sn}_1$  also possess Li sharing 14 fold  $\text{Li}_{14}\text{Sn}$  elongated hexagonal bipyramid with Sn atom located at the center position (Fig.2(vii)). The Li-Sn distance in the cage is found to vary from  $2.83 \text{ \AA}$  to  $3.38 \text{ \AA}$  while Sn-Sn shortest distance is determined as  $\sim 4.83 \text{ \AA}$ . The high pressure  $P\bar{1}$ - $\text{Li}_7\text{Sn}_1$  structure consists of face-sharing 16-fold  $\text{Li}_{16}\text{Sn}$  octadecahedrons (Fig.2(viii)). Here the coordination number of Sn atoms increases from 14 to 16 having Li-Sn distance in the range of  $2.65 \text{ \AA}$  to  $2.85 \text{ \AA}$  at 20 GPa pressure (Fig. S12 and Table T11 in SI).

## C. Volume Expansion

It is known that the massive structural change and volume expansion of the order of  $\sim 240\%$  during lithiation/delithiation of Sn lead to severe cracking and pulverization of the electrode and capacity fading, which restricts the use of Sn as an anode material in commonly used Li-ion batteries.[8, 10, 11] However, application of pressure can help in reducing this drastic change in volume during lithiation/delithiation.[16] It is evident from Figure 3(a) that volume expands quadratically with the increase in Li-concentration, which is in agreement with the results of Li et al.,[67] but simultaneously, it also contracts with the increase in pressure. For example, as compared to  $\beta$ -Sn the volume of the most stable  $\text{Li}_{13}\text{Sn}_5$  compound increases by  $\sim 131\%$ ,  $101\%$ ,  $84\%$ , and  $62\%$ , when the pressure is 1 atm, 5, 10, and 20 GPa, respectively. Similarly, as compared to the volume of  $\beta$ -Sn at 1 atm pressure, the respective increase in the volume of Li-rich phases like  $\text{Li}_{17}\text{Sn}_4/\text{Li}_5\text{Sn}_1/\text{Li}_7\text{Sn}_1$  is observed to be  $\sim 240/280/425\%$ ,  $191/220/334\%$ ,  $165/190/288\%$ ,  $130/150/230\%$ , when the pressure is 1 atm, 5, 10, and 20 GPa. Thus, it is clear from our calculations that, in general, pressure reduces the volume expansion as expected, and in particular, a pressure of 20 GPa helps in reducing this volume expansion by roughly half as compared to 1 atm pressure. This also leads to increase in energy density. Pressure can be efficiently generated in Li-Sn compounds by chemical doping of an impurity, by a proper selection of substrate material such that it induces pressure due to lattice mismatch on Sn anode deposited on it or, by imposing pressure externally, to obtain pressure induced Li-rich phases. However, using directly such high pressure (of the order of GPa) may not be suitable for battery applications and therefore, we propose to use high pressure phases quenched to ambient pressure. We believe that this may still prove useful in producing relatively less change in volume during lithiation/delithiation process and providing better mechanical integrity, which is essentially required to improve performance of Li-Sn batteries.

## D. Electro-chemical Properties

**Gravimetric Capacity:** The gravimetric capacity of all Li-Sn compounds explored in this work are tabulated in Table I. Since the gravimetric capacity is directly proportional to the concentration of Li (eq.3), it increases with the increase in Li concentration. Interestingly our calculations predict several novel pressure-induced high capacity Li-rich compositions ( $\text{Li}_3\text{Sn}_1$ ,  $\text{Li}_4\text{Sn}_1$ ,  $\text{Li}_5\text{Sn}_1$ , and  $\text{Li}_7\text{Sn}_1$ ) which are although metastable at ambient pressure, but should be synthesizable because of non-existence of any negative frequencies in phonon dispersion curve at 1 atm (Fig.S1 in SI).

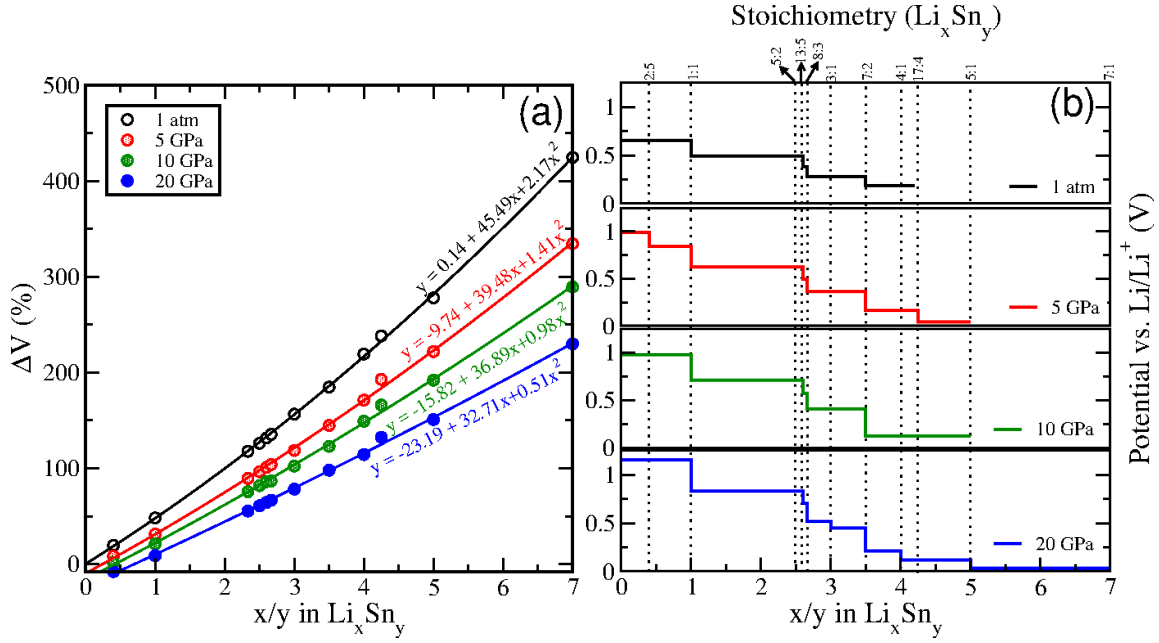


Figure 3. (a) Volume expansion of Li-Sn compounds at 1 atm, 5, 10, and 20 GPa pressure with respect to the volume of  $\beta$ -Sn ( $I_{41}/\text{amd}$ ) at 1 atm pressure. (b) Potential-composition curves at 1 atm, 5, 10, and 20 GPa pressure for stable Li-Sn compounds that lie on the convex hull in Fig.1(a).

Specifically,  $\text{Li}_5\text{Sn}_1$  and  $\text{Li}_7\text{Sn}_1$  are the two compounds that exhibit higher specific capacity ( $\sim 1129$  and  $\sim 1580 \text{ mAh g}^{-1}$ ) than yet known most lithiated  $\text{Li}_{17}\text{Sn}_4$  phase ( $\sim 960 \text{ mAh g}^{-1}$ ). In fact,  $\text{Li}_7\text{Sn}_1$  exhibit much higher capacity,  $\sim 5$  times than  $\text{LiC}_6$  ( $\sim 372 \text{ mAh/g}$ ) and  $\gtrsim 1.5$  times than  $\text{Li}_{17}\text{Sn}_4$ . Since pressure does not affect the capacity directly, our results suggest that a Li-ion battery with higher capacity might be formed if the quenched high pressure – high capacity phase is used as the pre-lithiated anode material.

**Li-insertion Voltage:** Average lithium insertion voltages in Sn anode of Li-ion battery are presented in Figure 3(b) for the 1 atm, 5, 10, and 20 GPa pressure values. These are calculated using DFT total energies, assuming that the displaced charge is due to Li and that the reaction proceeds sequentially through the phases lie on the tie-lines of the convex hull corresponding to respective pressure value.[51] On analysing Figure 3(b), we found that the average Li-insertion voltage increases with the increase in pressure. At 1 atm pressure the voltage drops from  $\sim 0.65 \text{ V}$  to  $0.18 \text{ V}$ , when Sn is fully lithiated to  $\text{Li}_{17}\text{Sn}_4$  phase. Note that as per our calculations, at 1 atm pressure (and 0 K),  $\text{Li}_2\text{Sn}_5$  does not lie on the tie-line of the convex hull, thus, it is not included in the voltage-composition curve for the 1 atm pressure. The 5 GPa curve includes two new phases, viz.  $\text{Li}_2\text{Sn}_5$  and  $\text{Li}_5\text{Sn}_1$ , which increases the voltage range by  $\sim 50\%$ , as the voltage drops from  $1 \text{ V}$  to  $0.04 \text{ V}$ , when Sn is lithiated to  $\text{Li}_5\text{Sn}_1$  phase. Compared to 5 GPa, the voltage decreases slightly in case of 10 GPa, as  $\text{Li}_2\text{Sn}_5$  and  $\text{Li}_{17}\text{Sn}_4$  become unstable at this pressure value. However, the voltage again increases to  $1.15 \text{ V}$  at 20 GPa as several Li-rich phases like  $\text{Li}_5\text{Sn}_2$ ,  $\text{Li}_3\text{Sn}_1$ ,  $\text{Li}_4\text{Sn}_1$ ,  $\text{Li}_5\text{Sn}_1$ , and  $\text{Li}_7\text{Sn}_1$  become stable, which increases the number of successive two-phase reactions. Thus, the application of pressure not just increases the energy density but also provides relatively higher insertion voltage which is desired to make the battery safer, as it reduces the chance of lithium plating that results into dendrites causing short-circuit in the cell.[42]

### E. Mechanical properties of Li-Sn compounds.

A composition (having negative formation enthalpy) which does not lie on the tie-line of the convex hull can be regarded as metastable, only and only if, it satisfies the criteria of both, dynamical and mechanical stability. In above section we have shown that all the new phases (stable or metastable) revealed in this work are dynamically stable by calculating their phonon dispersion curves (See Fig.S1 & S2 in SI). Now to check the mechanical stability of the same, we used the Born criteria of mechanical stability described by Wu et al. and Mouhat et al.,[68, 69] which highly depends on the symmetry of the crystal. To check the criteria, the elastic constants of all thermodynamically stable and metastable Li-Sn compounds at pressure value of 1 atm, 5, 10, and 20 GPa are calculated (Table T3, T4, T5, & T6 of SI). Using the elastic constants corresponding to the particular composition and pressure in the Born criteria,

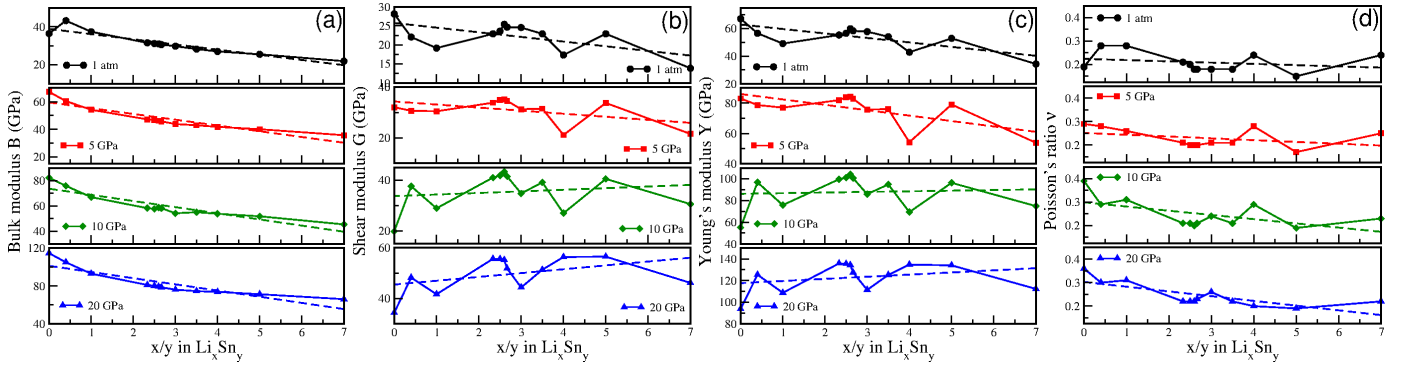


Figure 4. (a) Bulk modulus (B), (b) Shear modulus (G), (c) Young's modulus (Y), and (d) Poisson's ratio ( $\nu$ ) of Li-Sn compounds with respect to lithium fraction  $x/y$  in  $\text{Li}_x\text{Sn}_y$  at pressure value of 1 atm, 5, 10, and 20 GPa.

it is interestingly found that all examined compounds are mechanically stable. This further supports our prediction for the possible existence of newly predicted compounds in the Li-Sn binary system.

One of the major bottleneck of using Sn anode is the elastic softening and mechanical degradation with lithiation, which leads to electrode damage and fracture. In order to see the influence of pressure on mechanical properties, we examined the elastic properties of all investigated Li-Sn stoichiometries at various pressure values. Such studies may prove helpful in restricting the failure mechanism of Li-ion batteries during charging-discharging process. However, it is noteworthy here that DFT calculated elastic constants are for the single crystal, while the Li-Sn compounds formed during lithiation in Li-ion batteries, are usually in polycrystalline micro-structures state.[70] Thus, in order to characterize the mechanical performance of Li-Sn compounds, we calculate the isotropic elastic constants for a polycrystalline aggregate by averaging the computed anisotropic single crystal elastic constants over all possible orientations of the grains in a polycrystal. The continuum model based on Reuss and Voigt approaches are explicitly used for such studies (see SI for more details).

The orientation averaged bulk modulus, Young's modulus, shear modulus, and Poisson's ratio with increasing Li concentration in Sn are presented in Figure 4. It can be seen that bulk, shear, and Young's moduli depend significantly on Li concentration, as well as pressure. Mostly these moduli decrease with the increase in Li/Sn fraction ( $x/y$ ), showing elastic softening in the Li-rich phases, in agreement with previous theoretical and experimental findings.[70–72] However, with the increase in pressure the average value of these moduli increases substantially. While, as compared to Sn at ambient pressure a decrease of  $\sim 50\%$  is noticed in the bulk modulus of most Li-rich phase,  $\text{Li}_7\text{Sn}_1$ , this difference gets reduced to  $\sim 40\%$  at high pressure. Moreover, instead of an approximate linear decrease, shear and Young's moduli show a linear increase with the increase in the Li-concentration beyond  $\sim 10$  GPa. This indicates a pressure induced relative stiffness in each phase, which strengthens the Li-Sn phases at high pressure as compared to ambient pressure. Our calculated Poisson's ratio for all investigated compounds, lies between 0.1 to 0.4 (i.e., well within the limit of a stable and linear elastic material), further supports our conclusion, as it is evident from Fig. 4(d) that the relative value of Poisson ratio for most of the investigated materials increases with the increase in pressure.

Table II. Calculated universal anisotropy index ( $A^U$ ) of Li, Sn, and Li-Sn compounds at 1 atm, 5, 10, 20 GPa pressure.

Pressure	$A^U$												
	Sn	$\text{Li}_2\text{Sn}_5$	$\text{Li}_1\text{Sn}_1$	$\text{Li}_7\text{Sn}_3$	$\text{Li}_5\text{Sn}_2$	$\text{Li}_{13}\text{Sn}_5$	$\text{Li}_8\text{Sn}_3$	$\text{Li}_3\text{Sn}_1$	$\text{Li}_7\text{Sn}_2$	$\text{Li}_4\text{Sn}_1$	$\text{Li}_5\text{Sn}_1$	$\text{Li}_7\text{Sn}_1$	Li
1 atm	1.53	0.59	0.39	3.69	2.80	2.87	2.96	2.09	1.70	6.17	0.33	6.26	7.93
5 GPa	0.89	0.39	0.15	2.56	2.21	2.55	2.39	2.01	1.54	9.88	0.13	3.69	13.87
10 GPa	1.88	0.61	1.37	2.36	1.92	2.31	2.33	2.68	1.33	7.32	0.12	0.85	2.14
20 GPa	1.77	0.64	0.98	2.01	1.79	2.09	2.34	2.70	1.14	0.56	0.14	0.21	1.41

To further check the mechanical robustness of compressed Li-Sn compounds, we also examined the influence of elastic anisotropy with respect to pressure on Li-Sn compounds, since it is well known that due to anisotropy of materials micro-cracks can be induced in Sn anode during charging and discharging.[71] The universal anisotropy index ( $A^U$ ), proposed by Ranganathan et.al.,[73] is used in this work to quantify the elastic anisotropy:

$$A^U = 5 \frac{G_V}{G_R} + \frac{B_V}{B_R} - 6. \quad (4)$$

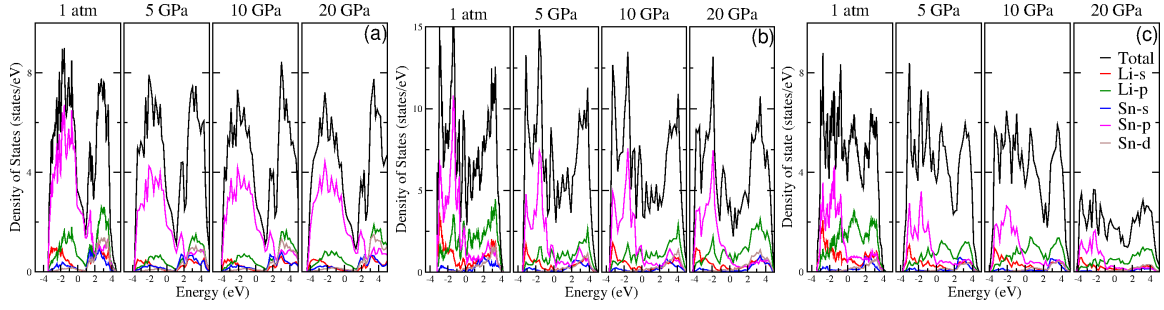


Figure 5. Total and partial density of states (DOS) of (a)  $\text{Li}_8\text{Sn}_3$ , (b)  $\text{Li}_5\text{Sn}_1$ , and (c)  $\text{Li}_7\text{Sn}_1$  at 1 atm, 5, 10, and 20 GPa pressure.

Zero value of  $A^U$  indicates the local isotropy, while, the more deviation of the parameter from zero represents more elastic anisotropy of the crystalline structure. The calculated elastic anisotropy index for different pressure values listed in Table II, show an extremely opposite trend for the two end members of the Li-Sn system at 1 atm and 5 GPa pressure. While,  $\alpha$ -Sn at 1 atm and  $\beta$ -Sn at 5 GPa are nearly isotropic with  $A^U = 1.53$  and 0.89, respectively, a strong anisotropic property is found for b.c.c. Li ( $A^U = 7.93$  at 1 atm and 13.87 at 5 GPa). The anisotropic behaviour of these two elements are in good agreement with the previous theoretical and experiment results.[71, 73–75] However on the contrary, the f.c.c. Li at high pressure is quite isotropic ( $A^U = 2.14 - 1.14$ ) and it's isotropic nature improves with the increase in pressure. It should also be noticed that at ambient pressure, the medium intercalated-lithium phases ( $1 < x < 3.5$ ) are moderately anisotropic, while, except  $\text{Li}_5\text{Sn}_1$ , the Li-rich phases ( $3.5 < x \leq 7$ ) are highly anisotropic. One can see from Table II that the value of  $A^U$  for two of our newly predicted metastable compounds, i.e.,  $\text{Li}_4\text{Sn}_1$  and  $\text{Li}_7\text{Sn}_1$ , at ambient pressure reaches close to the value of b.c.c. Li, with  $A^U = 6.17$  and 6.26, respectively, while,  $\text{Li}_5\text{Sn}_1$  is found to be most isotropic among all other Li-Sn compounds with anisotropy index of 0.33. This is not very surprising as a similar trend was also noticed by Zhang et.al.,[71] as they observed  $\text{Li}_{17}\text{Sn}_4$  (a closer system to  $\text{Li}_5\text{Sn}_1$ ) to be more isotropic than any other Li-Sn phases with  $A^U \sim 0$ . The most important thing to notice is that the isotropy improves with the increase in pressure and even the Li-rich compounds like  $\text{Li}_4\text{Sn}_1$  and  $\text{Li}_7\text{Sn}_1$  become highly isotropic (equivalent to  $\text{Li}_5\text{Sn}_1$ ) at high pressure. These results clearly reveal that pressure improves the mechanical properties of Li-Sn compounds and thus, we strongly believe that the quenched high pressure phases may also exhibit superior mechanical properties, which can help in resolving the current problem of fracture and pulverization in Sn anode.

## F. Electronic Properties and Chemical Bonds.

Electronic properties, in general, and electrical conductivity, in particular, of any electrode material also play crucial role in determining performance of a Li-ion battery. Fig.S11 in SI depicts the calculated total electronic density of states (DOS) along with the atom resolved partial density of states (PDOS) of all the phases at 1 atm. The crossover of several bands at Fermi level ( $E_F$ , set to zero) indicate all Li-Sn compounds to exhibit metallic nature, thus, providing a better electrical conductivity. For most of the Li-Sn phases, the PDOS show a large overlap between Sn-5p and Li-2s and/or Li-2p states at the Fermi level, which illustrates the charge transfer from Li-2s and/or Li-2p to Sn-5p. One can see that the main contribution to total DOS near  $E_F$  comes from the Sn-5p state but, as expected this gets weakened with the increase in Li-concentration, which is also in agreement with the work of Zhang et al.[71] on Li-Sn systems at ambient conditions. Moreover, this is also very similar to what is observed recently by Zhang et al.[33] and Yang et al.[76] for Li-Si and Li-Au systems at high pressure, respectively. Finally, in Li-rich phases where  $x \geq 4$ , Li-2s and Li-2p states dominate and provide major contribution to the total DOS near  $E_F$ , as compared to Sn-5p state, owing to the exceptionally high concentration of Li (Fig.S11 in SI). In order to determine the effect of pressure on density of states, we present DOS for three of the yet unknown/unexplored compounds ( $\text{Li}_8\text{Sn}_3$ ,  $\text{Li}_5\text{Sn}_1$ , and  $\text{Li}_7\text{Sn}_1$ ) at different pressure values in Fig.5. It is evident from the figure that the nature of DOS is mainly insensitive to the applied pressure. The application of pressure in GPa though decreases the intensity of peaks (density/states) as compared to 1 atm pressure, but other than that no distinct change is noticed for any particular phase within the pressure value of 5–20 GPa.

In order to relate the chemical, electronic, and mechanical properties, the average electronegativity (EN) and the net charge on Li and Sn atoms for each  $\text{Li}_x\text{Sn}_y$  compound are also calculated. The average metallic EN is calculated using formula:  $\frac{x(\text{EN})_{\text{Li}} + y(\text{EN})_{\text{Sn}}}{x + y}$ , where  $(\text{EN})_{\text{Li}}$  and  $(\text{EN})_{\text{Sn}}$  are metallic EN values of Li and Sn, respectively, and  $x$



and  $y$  are the numbers of Li and Sn atoms per chemical formula. EN describes the ability of an atom or ion to attract bonding valence electrons, and thus, the average EN of two bonded atoms can well reflect the strength or nature of the chemical bonds.[67] A large value of average EN reflects a strong covalent bonding (Sn-Sn), while intermediate to low values indicate weak ionic (Li-Sn) and metallic bonds (Li-Li), respectively. It is evident from the above formula that average EN does not depend on pressure but it is found that it decreases monotonically with the increase in Li-concentration, that also explains the elastic softening in Li-rich compounds. The average EN for Sn,  $\text{Li}_2\text{Sn}_5$ ,  $\text{Li}_1\text{Sn}_1$ ,  $\text{Li}_7\text{Sn}_3$ ,  $\text{Li}_5\text{Sn}_2$ ,  $\text{Li}_{13}\text{Sn}_5$ ,  $\text{Li}_8\text{Sn}_3$ ,  $\text{Li}_3\text{Sn}_1$ ,  $\text{Li}_7\text{Sn}_2$ ,  $\text{Li}_4\text{Sn}_1$ ,  $\text{Li}_{17}\text{Sn}_4$ ,  $\text{Li}_5\text{Sn}_1$ , and  $\text{Li}_7\text{Sn}_1$  is calculated to be 2.860, 2.227, 1.753, 1.310, 1.279, 1.261, 1.250, 1.200, 1.138, 1.089, 1.068, 1.015, 0.923, and 0.646, respectively.

Bader charge further justifies the increase of ionic character in Li-Sn compounds with higher Li-concentration. In agreement with previous calculations,[70] our calculations show that when  $x < 5$  in  $\text{Li}_x\text{Sn}$ , all Li atoms donate electrons to Sn atoms and acquire  $\sim +1$  charge, while Sn atoms take 1 – 4 electrons, leading to a net charge of roughly  $-1$  to  $-4$  compared to pristine Sn, depending on the amount of Li and neighboring Sn atoms, as well as on the anisotropy of the phase.[70] For example, in  $\text{Li}_8\text{Sn}_3$ , Sn atoms forming dumbbell exhibit a charge of -1.96, while monomer of Sn atoms are found to have -2.68 charge at ambient pressure (Table 12 of SI). Likewise,  $\text{R3m-Li}_4\text{Sn}_1$  that contains isolated Sn atoms, exhibit  $\sim -3.28$  charge on each Sn atom at ambient pressure. On the other hand, in  $\text{I4/m-Li}_4\text{Sn}_1$ , there are two types of Sn atoms, one surrounded by 8 Li atoms, carrying charge of  $-3.38$  while, others that are enclosed by 7 Li atoms possess -3.04 charge at 20 GPa pressure (Table 13 in SI). Well, in principle, Li can donate 1 electron to acquire  $+1$  charge and Sn can accept upto 4 electrons to attain maximum of  $-4$  charge, to form most lithiated Sn compounds like  $\text{Li}_4\text{Sn}_1$  or  $\text{Li}_{17}\text{Sn}_4$ . However, our calculations reveal compounds with higher concentration of Li, such as,  $\text{Li}_5\text{Sn}_1$  and  $\text{Li}_7\text{Sn}_1$ , which suggest possibility of Sn to earn  $-5$  and  $-7$  charge, respectively. But, this seems difficult considering octet rule. Here, our Bader charge analysis helped us to resolve this ambiguity by providing the charge distribution in such Li-rich materials. Interestingly, our calculations illustrate that instead of Sn acquiring more than  $-4$  charge, few of the Li atoms accept electrons and becomes negatively charged (Table 12 & 13 of SI). In  $\text{Li}_5\text{Sn}_1$ , Sn exhibits net charge of  $\sim -3.6$ , while 36 Li atoms possess  $\sim +0.82$  and 4 Li atoms acquire  $-0.03$  charge. Likewise, in  $\text{Li}_7\text{Sn}_1$ , out of 28 Li atoms in the conventional cell, 8 Li accept electrons to become negatively charge with charge  $\sim 0.05 - 0.28$ , at ambient pressure (see Table 12 of SI). This result is not at all surprising as the same has been noticed in the case of  $\text{NaCl}_7$ [31] and  $\text{KCl}_7$ [77], where one of the Cl atom acquires +ve charge to maintain charge neutrality. The negative charge on few of the Li also explains the reason of sudden increase in the contribution of Li-states to the total DOS near Fermi-level. Moreover, except  $\text{Li}_7\text{Sn}_1$ , the net charge on each atom is not found to be much sensitive to pressure. In  $\text{Li}_7\text{Sn}_1$ , with application of moderate pressure instead of 8 Li atoms at ambient pressure, only 4 atoms are found to have negative charge, but at the same time the net charge increases from  $\sim -0.28$  to  $\sim -0.79$ . This possibly happens due to reduction in anisotropy and phase change in  $\text{Li}_7\text{Sn}_1$  at 20 GPa.

#### IV. CONCLUSIONS

First-principles evolutionary algorithm based simulations are performed to study the lithiation of Sn anode at ambient and moderately high pressure of  $\leq 20$  GPa. At ambient pressure, our calculations not only validate the well known existing Li-Sn compositions by correctly predicting their phases, but also revealed one of the most stable and yet unexplored Li-Sn compound— $\text{Li}_8\text{Sn}_3$ , together with several Li-rich metastable stoichiometries. Other than augmenting a new phase in ambient pressure phase diagram, our calculations also highlight the role of pressure (compressive strain) in stabilizing several unknown Li-rich compounds to enrich the moderate pressure phase diagram with compositions like  $\text{Li}_3\text{Sn}_1$ ,  $\text{Li}_4\text{Sn}_1$ ,  $\text{Li}_5\text{Sn}_1$ , and  $\text{Li}_7\text{Sn}_1$ . Interestingly, discovery of  $\text{Li}_5\text{Sn}_1$  and  $\text{Li}_7\text{Sn}_1$  surpasses the theoretical gravimetric capacity of existing highest lithiated phase,  $\text{Li}_{17}\text{Sn}_4$ , and suggests an option to enhance the capacity of a Li-Sn battery by almost 1.5 times ( $\sim 1580 \text{ mAh g}^{-1}$ ) as compared to  $\text{Li}_{17}\text{Sn}_4$ , by using quenched high pressure – high capacity phase as the pre-lithiated anode material. Most importantly, besides providing a rich structural diversity for the Li-Sn system, our calculations also suggest that application of pressure helps in reducing the volume expansion by  $\sim 50\%$  at 20 GPa and improving the mechanical properties by substantially increasing the average value of bulk, shear, and Young's moduli as compared to ambient pressure. This will certainly help in overcoming the deformation and fracture of Sn anode during charge-discharge process. Moreover, the electronic properties are found to be less sensitive to pressure, thus, essentially providing a good electrical conductivity even at high pressure. Over all our study elucidates pressure to be an extra variable for improving the mechanical and electrochemical properties of Li-Sn compounds, which can help in providing a new dimension to the research in Li-Sn batteries. We expect our predictions will provide basis for future experimental investigations of the Li-Sn system.

## ACKNOWLEDGMENTS

Authors thank Prof. Artem R. Oganov for fruitful discussion and critical reading of this manuscript. P. J. would also like to acknowledge the support provided by Grant No. SR/FTP/PS-052/2012 from Department of Science and Technology (DST), Government of India. The high performance computing facility and workstations available at the School of Natural Sciences, Shiv Nadar University, was used to perform all calculations.

- 
- [1] N. Nitta, F. Wu, J. Lee, and G. Yushin, *Materials Today* **18**, 252 (2015).
  - [2] J.-M. Tarascon and M. Armand, *Nature* **414**, 359 (2001).
  - [3] V. Etacheri, R. Marom, R. Elazari, G. Salitra, and D. Aurbach, *Energy Environ. Sci.* **4**, 3243 (2011).
  - [4] K. Kang, Y. S. Meng, J. Bréger, C. P. Grey, and G. Ceder, *Science* **311**, 977 (2006).
  - [5] M. Armand and J.-M. Tarascon, *Nature* **451**, 652 (2008).
  - [6] M. S. Whittingham, *Chem. Rev.* **114**, 11414 (2014).
  - [7] C.-M. Park, J.-H. Kim, H. Kim, and H.-J. Sohn, *Chem. Soc. Rev.* **39**, 3115 (2010).
  - [8] W.-J. Zhang, *Journal of Power Sources* **196**, 13 (2011).
  - [9] M. N. Obrovac and V. L. Chevrier, *Chem. Rev.* **114**, 11444 (2014).
  - [10] H. Tian, F. Xin, X. Wang, W. He, and W. Han, *Journal of Materiomics* **1**, 153 (2015).
  - [11] C.-Y. Chou, H. Kim, and G. S. Hwang, *The Journal of Physical Chemistry C* **115**, 20018 (2011).
  - [12] P. Johari, Y. Qi, and V. B. Shenoy, *Nano Lett.* **11**, 5494 (2011).
  - [13] D. Larcher, S. Beattie, M. Morcrette, K. Edstrom, J.-C. Jumas, and J.-M. Tarascon, *J. Mater. Chem.* **17**, 3759 (2007).
  - [14] Y. Idota, T. Kubota, A. Matsufuji, Y. Maekawa, and T. Miyasaka, *Science* **276**, 1395 (1997).
  - [15] S.-H. Na and C.-H. Park, *Journal of the Korean Physical Society* **56**, 494 (2010).
  - [16] Z. Zeng, Q. Zeng, N. Liu, A. R. Oganov, Q. Zeng, Y. Cui, and W. L. Mao, *Adv. Energy Mater.* **5**, 1500214 (2015).
  - [17] F. Robert, P. Lippens, J. Olivier-Fourcade, J.-C. Jumas, F. Gillot, M. Morcrette, and J.-M. Tarascon, *Journal of Solid State Chemistry* **180**, 339 (2007).
  - [18] R. Dunlap, D. Small, D. MacNeil, M. Obrovac, and J. Dahn, *Journal of Alloys and Compounds* **289**, 135 (1999).
  - [19] D. Hansen and L. J. Chang, *Acta Cryst.* **B25**, 2392 (1969).
  - [20] W. Müller and H. Schäfer, *Z. Naturforsch.* **28b**, 246 (1973).
  - [21] W. Blase and G. Cordier, *Zeitschrift für Kristallographie* **193**, 317 (1990).
  - [22] W. Müller, *Z. Naturforsch.* **29b**, 304 (1974).
  - [23] U. Frank, W. Müller, and H. Schäfer, *Z. Naturforsch.* **30b**, 1 (1975).
  - [24] U. Frank and W. Müller, *Z. Naturforsch.* **30b**, 316 (1975).
  - [25] U. Frank, W. Müller, and H. Schäfer, *Z. Naturforsch.* **30b**, 6 (1975).
  - [26] G. Goward, N. Taylor, D. Souza, and L. Nazar, *Journal of Alloys and Compounds* **329**, 82 (2001).
  - [27] C. Lupu, J.-G. Mao, J. Rabalais, A. Guloy, and J. J. Richardson, *Inorganic Chemistry* **42**, 3765 (2003).
  - [28] E. Gladyshevskii, G. Oleksiv, and K. P.I., *Kristallografiya* **9**, 338 (1964).
  - [29] T. Matsuoka and K. Shimizu, *Nature* **458**, 186 (2009).
  - [30] F. Vnuk, A. De Monte, and R. W. Smith, *Journal of Applied Physics* **55**, 4171 (1984).
  - [31] W. Zhang, A. R. Oganov, A. F. Goncharov, Q. Zhu, S. E. Boulfelfel, A. O. Lyakhov, E. Stavrou, M. Somayazulu, V. B. Prakapenka, and Z. Konôpková, *Science* **342**, 1502 (2013).
  - [32] L. A. Stearns, J. Gryko, J. Diefenbacher, G. K. Ramachandran, and P. F. McMillan, *Journal of Solid State Chemistry* **173**, 251 (2003).
  - [33] S. Zhang, Y. Wang, G. Yang, and Y. Ma, *ACS Applied Materials & Interfaces* **8**, 16761 (2016).
  - [34] J. Zhao, Z. Lu, N. Liu, H.-W. Lee, M. M. T., and Y. Cui, *Nature Comm.* **5**, 5088 (2014).
  - [35] J. E. Cloud, Y. Wang, T. S. Yoder, L. W. Taylor, and Y. Yang, *Angewandte Chemie International Edition* **53**, 14527 (2014).
  - [36] A. Oganov and C. Glass, *J. Chem. Phys.* **124**, 244704 (2006).
  - [37] A. Oganov, A. O. Lyakhov, and M. Valley, *Acc. Chem. Res.* **44**, 227 (2011).
  - [38] A. O. Lyakhov, A. R. Oganov, H. Stokes, and Q. Zhu, *Comput. Phys. Commun.* **184**, 1172 (2013).
  - [39] C. J. Pickard and R. J. Needs, *Journal of Physics: Condensed Matter* **23**, 053201 (2011).
  - [40] S. Goedecker, *The Journal of Chemical Physics* **120**, 9911 (2004).
  - [41] W. W. Tipton, C. R. Bealing, K. Mathew, and R. G. Hennig, *Phys. Rev. B* **87**, 184114 (2013).
  - [42] A. J. Morris, C. P. Grey, and C. J. Pickard, *Phys. Rev. B* **90**, 054111 (2014).
  - [43] I. Valencia-Jaime, R. Sarmiento-Pérez, S. Botti, M. Marques, M. Amsler, S. Goedecker, and A. Romero, *Journal of Alloys and Compounds* **655**, 147 (2016).
  - [44] J. Badding, L. Parker, and D. Nesting, *Journal of Solid State Chemistry* **117**, 229 (1995).
  - [45] W. Sun, S. T. Dacek, S. P. Ong, G. Hautier, A. Jain, W. D. Richards, A. C. Gamst, K. A. Persson, and G. Ceder, *Science Advances* **2**, 1 (2016).
  - [46] G. Kresse and J. Furthmüller, *Phys. Rev. B* **54**, 11169 (1996).
  - [47] G. Kresse and J. Furthmüller, *Computational Materials Science* **6**, 15 (1996).

- [48] P. E. Blöchl, Phys. Rev. B **50**, 17953 (1994).
- [49] J. P. Perdew, K. Burke, and M. Ernzerhof, Phys. Rev. Lett. **77**, 3865 (1996).
- [50] A. Togo, F. Oba, and I. Tanaka, Phys. Rev. B **78**, 134106 (2008).
- [51] G. Ceder, M. Aydinol, and A. Kohan, Computational Materials Science **8**, 161 (1997).
- [52] R. Hill, Proceedings of the Physical Society. Section A **65**, 349 (1952).
- [53] M. Hanfland, I. Loa, K. Syassen, U. Schwarz, and K. Takemura, Solid State Communications **112**, 123 (1999).
- [54] J. B. Neaton and N. W. Ashcroft, Nature **400**, 141 (1999).
- [55] C. Yu, J. Liu, H. Lu, and J. Chen, Solid State Communications **140**, 538 (2006).
- [56] J. Barnett, R. Bennion, and H. T. Hall, Science **141**, 1041 (1963).
- [57] O. Genser and J. Hafner, Phys. Rev. B **63**, 144204 (2001).
- [58] J. E. Saal, S. Kirklin, M. Aykol, B. Meredig, and C. Wolverton, JOM **65**, 1501 (2013).
- [59] S. Kirklin, J. Saal, B. Meredig, A. Thompson, J. Doak, M. Aykol, S. Rühl, and C. Wolverton, npj Computational Materials **1**, 15010 (2015).
- [60] W. Gasior, Z. Moser, and W. Zakulski, Journal of Non-Crystalline Solids **205**, 379 (1996).
- [61] P. Lu, J.-S. Kim, H. Gao, J. Wu, D. Shao, B. Li, D. Zhou, J. Sun, D. Akinwande, D. Xing, et al., Phys. Rev. B **94**, 224512 (2016).
- [62] A. Darwiche, C. Marino, M. T. Sougrati, B. Fraisse, L. Stievenano, and L. Monconduit, Journal of the American Chemical Society **134**, 20805 (2012).
- [63] M. Thackeray, J. Vaughey, C. Johnson, A. Kropf, R. Benedek, L. Fransson, and K. Edstrom, Journal of Power Sources **113**, 124 (2003).
- [64] B. P. Alblas, W. v. d. Lugt, J. Dijkstra, and C. v. Dijk, Journal of Physics F: Metal Physics **14**, 1995 (1984).
- [65] Y. Lin, T. A. Strobel, and R. E. Cohen, Phys. Rev. B **92**, 214106 (2015).
- [66] A. Zalkin and W. J. Ramsey, The Journal of Physical Chemistry **60**, 234 (1956).
- [67] K. Li, H. Xie, J. Liu, Z. Ma, Y. Zhou, and D. Xue, Phys. Chem. Chem. Phys. **15**, 17658 (2013).
- [68] Z.-J. Wu, E.-J. Zhao, H.-P. Xiang, X.-F. Hao, X.-J. Liu, and J. Meng, Phys. Rev. B **76**, 054115 (2007).
- [69] F. Mouhat and F.-X. Coudert, Phys. Rev. B **90**, 224104 (2014).
- [70] M. E. Stournara, P. R. Guduru, and V. B. Shenoy, Journal of Power Sources **208**, 165 (2012).
- [71] P. Zhang, Z. Ma, Y. Wang, Y. Zou, W. Lei, Y. Pan, and C. Lu, RSC Adv. **5**, 36022 (2015).
- [72] J. Chen, S. J. Bull, S. Roy, H. Mukaibo, H. Nara, T. Momma, T. Osaka, and Y. Shacham-Diamand, Journal of Physics D: Applied Physics **41**, 025302 (2008).
- [73] S. I. Ranganathan and M. Ostoja-Starzewski, Phys. Rev. Lett. **101**, 055504 (2008).
- [74] R. A. Felice, J. Trivisonno, and D. E. Schuele, Phys. Rev. B **16**, 5173 (1977).
- [75] D. G. House and E. Vernon, British Journal of Applied Physics **11**, 254 (1960).
- [76] G. Yang, Y. Wang, F. Peng, A. Bergara, and Y. Ma, Journal of the American Chemical Society **138**, 4046 (2016).
- [77] W. Zhang, A. R. Oganov, Q. Zhu, Q. Zhu, E. Stavrou, and A. F. Goncharov, Scientific Reports **6**, 26265 (2016).